

Oscillations of dark solitons in trapped Bose-Einstein condensates

Dmitry E. Pelinovsky¹, D.J. Frantzeskakis², and P.G. Kevrekidis³

¹ *Department of Mathematics, McMaster University, Hamilton, Ontario, Canada, L8S 4K1*

² *Department of Physics, University of Athens, Panepistimiopolis, Zografos, Athens 15784, Greece*

³ *Department of Mathematics and Statistics, University of Massachusetts, Amherst MA 01003-4515, USA*

We consider a one-dimensional defocusing Gross–Pitaevskii equation with a parabolic potential. Dark solitons oscillate near the center of the potential trap and their amplitude decays due to radiative losses (sound emission). We develop a systematic asymptotic multi-scale expansion method in the limit when the potential trap is flat. The first-order approximation predicts a uniform frequency of oscillations for the dark soliton of arbitrary amplitude. The second-order approximation predicts the nonlinear growth rate of the oscillation amplitude, which results in decay of the dark soliton. The results are compared with the previous publications and numerical computations.

I. INTRODUCTION

Dark matter-wave solitons in atomic Bose–Einstein condensates (BECs) have many similarities with dark optical solitons in defocusing nonlinear media [1, 2]. Both entities are fundamental nonlinear excitations of the defocusing nonlinear Schrödinger (NLS) equation, describing the evolution of electric field envelopes in the context of optics, or of the order parameter (the condensate mean-field wavefunction) in the context of atomic BECs. Dark matter-wave solitons were observed in a series of experiments carried out with BECs confined in external parabolic magnetic trapping potentials [3, 4, 5], and have inspired subsequent investigations of their stability and dynamics. In particular, if a dark (black) soliton is initially placed exactly at the center of the magnetic trap, it remains standing, while if it is misplaced, it starts oscillating near the center of the trap. In this respect, there has been a recent interest in theoretical studies concerning the frequency and amplitude of these oscillations, and especially on their dependence on the velocity and amplitude parameters of dark solitons.

Preliminary studies of small-amplitude oscillations of dark solitons were reported in [6, 7] by using the collective coordinate approach and assumptions of the soliton’s adiabatic dynamics. The frequency of oscillations obtained in [6, 7] was found to mismatch the correct frequency as explained in [8, 9, 10]. The main reason for discrepancy of results of [6, 7] is the use of the center-of-mass quantity (the Ehrenfest Theorem), as the integral quantity can change due to radiation from dark soliton [10]. Another integral quantity (the renormalized power invariant) was used in [10] (based on results of [11]), but the perturbation theory led to many correction terms in the main equations and relatively poor agreement with numerical simulations (see, e.g., Fig. 1 in [10]).

Another version of the perturbation theory for dark solitons can be developed with the use of the renormalized momentum [12] and can be adapted to incorporate radiative effects on the adiabatic dynamics of dark solitons [13]. This version of the perturbation theory relies on the completeness of eigenfunctions of the linearization problem established in [14, 15]. A recent application of

the perturbation theory, also accounting for radiative effects, has been reported in [16] for dark solitons in the presence of linear gain and two-photon absorption. The frequency of small-amplitude oscillations of dark solitons near the center of the trapping potential (and additional localized impurities) can be found from an integration of the renormalized momentum [9] in a much simpler form, as compared to the one presented in [10].

Other integral invariants have also been used to study the adiabatic dynamics of dark solitons, e.g. the boundary-layer integral for the corresponding hydrodynamic equations [8] and the energy (Hamiltonian) of the dark soliton [17]. Oscillations of dark solitons were also studied in the shallow soliton limit with the use of the Korteweg–de Vries (KdV) approximation [18]. Surprisingly enough, it was found that the frequency of oscillations of dark solitons does not depend on the soliton amplitude [17], or, in other words, the frequency of oscillations remained the same in the limits of black and shallow solitons [10, 18].

Recent numerical studies of oscillations of dark solitons in parabolic and other external traps were reported in [19, 20, 21]. It was found that the dark solitons emit radiation (in the form of sound waves) due to oscillations. If radiation escapes the trap (as in the case of a tight dimple trap [19], or in an optical lattice potential [21]), the energy (momentum) of the dark soliton changes, resulting in the growth of the oscillation amplitude and the decay of the soliton amplitude. A phenomenological explanation of the radiative decay of the soliton energy and the quadratic dependence of the energy decay rate on the soliton acceleration was proposed in [19, 20], based on the earlier analysis of [13]. However, the authors of [13] consider instability-induced dynamics of dark solitons in a homogeneous system, which is a different problem from dynamics of dark solitons in a trapped condensate.

Further variants of the problem include oscillations of ring dark solitons and vortex necklaces in two dimensions (i.e., for “pancake” BECs) [22], dynamics of shallow dark solitons in a gas of hard core bosons (the so-called Tonks–Girardeau gas which, in mean-field picture, is described by a quintic nonlinear Schrödinger equation) [23], parametric driving of dark solitons by periodically modulated

Gaussian paddles [24], and scattering of a dark soliton on a finite size obstacle [25]. It should be mentioned that the technique presented in [24] may pave the way for observing long-lived oscillating dark matter-wave solitons in future BEC experiments.

The present paper deals with the oscillations of a dark soliton in a BEC confined in a parabolic trap, as well as the inhomogeneity-induced emission of radiation. Our analytical approach relies on a systematic asymptotic multi-scale expansion method, based on ideas of [12, 13], as well as the perturbation theory for dark solitons [14, 15]. We prove that the main equation of motion for adiabatic dynamics of dark solitons of any amplitude is given by the harmonic oscillator equation with a constant frequency. Additionally, we account for radiation escaping the dark soliton and compute the nonlinear growth rate of the oscillation amplitude versus the amplitude of a dark soliton. Our results give a systematic basis for analysis of the dynamics of dark solitons in other systems. The analytical results are found to be very similar to the ones reported in recent studies [17, 21], except that a regular asymptotic technique, based on the explicit small parameter of the problem, replaces previous qualitative estimates based on numerical observations. Furthermore, we show why a formal application of the perturbation theory fails to incorporate the correct dependence of frequency of dark soliton oscillations.

The paper is organized as follows. Section 2 formulates the problem and reports the main results. Section 3 describes the asymptotic limit for the ground state of the parabolic potential. Section 4 gives a transformation of the Gross-Pitaevskii (GP) equation to the regularly perturbed nonlinear Schrödinger (NLS) equation. Section 5 contains the analysis of the perturbed NLS equation up to the first-order and second-order corrections. Section 6 reviews the formal application of perturbation theory to the GP equation and the previous results. Section 7 concludes the paper.

II. MODEL AND MAIN RESULTS

At low temperatures, the dynamics of a repulsive quasi-one-dimensional BEC, oriented along the x -axis, can be described by the following effective one-dimensional (1D) GP equation (see, e.g., [26])

$$i\hbar\psi_t = -\frac{\hbar^2}{2m}\psi_{xx} + V(x)\psi + g|\psi|^2\psi, \quad (1)$$

where subscripts denote partial derivatives, $\psi(x, t)$ is the mean-field BEC wavefunction, m is the atomic mass, and the nonlinearity coefficient g (accounting for the interatomic interactions) has an effective 1D form, namely $g = 2\hbar a\omega_\perp$, where a is the s-wave scattering length and ω_\perp is the transverse-confinement frequency. Additionally, the external potential $V(x)$ is assumed to be the usual harmonic trap, i.e., $V(x) = m\omega_x^2 x^2/2$, where ω_x is the confining frequency in the axial direction.

To reduce the original GP equation (1) to a dimensionless form, x is scaled in units of the fluid healing length $\xi = \hbar/\sqrt{n_0 g m}$ (which also characterizes the width of the dark soliton), t in units of ξ/c (where $c = \sqrt{n_0 g/m}$ is the Bogoliubov speed of sound), the atomic density $n \equiv |\psi|^2$ is rescaled by the peak density n_0 , and energy is measured in units of the chemical potential of the system $\mu = gn_0$. This way, the following normalized GP equation is readily obtained,

$$iu_t = -\frac{1}{2}u_{xx} + \epsilon^2 x^2 u + |u|^2 u, \quad (2)$$

where the parameter $\epsilon \equiv (2\sqrt{2}an_0)^{-1}(\omega_x/\omega_\perp)$ determines the magnetic trap strength and $u(x, t) \in \mathbb{C}$. Let us assume realistic experimental parameters for a quasi-1D repulsive condensate containing $N \sim 10^3$ – 10^4 atoms and with peak atomic density $n_0 \approx 10^8 \text{ m}^{-3}$. Then, as the scattering length a is of order of a nanometer (e.g., $a = 5.8 \text{ nm}$ or $a = 2.7 \text{ nm}$ for a ^{87}Rb or ^{23}Na condensate), and the ratio of the confining frequencies (for such a quasi-1D setting) is $\omega_x/\omega_\perp \sim 1/200$, it turns out that the magnetic trap strength ϵ is typically $\text{O}(10^{-2})$. Thus, ϵ is a natural small parameter of the problem.

When $\epsilon = 0$, the defocusing GP equation (2) has the exact solution for the dark soliton:

$$u_{\text{ds}}(x, t) = [k \tanh(k(x - vt - s_0)) + iv] e^{-it + i\theta_0}, \quad (3)$$

where $k = \sqrt{1 - v^2} < 1$ is the amplitude of the dark soliton (with respect to the continuous-wave background), $|v| < 1$ is the velocity parameter, and $(s_0, \theta_0) \in \mathbb{R}^2$ are arbitrary parameters of the position and phase. Since

$$|u_{\text{ds}}|^2 = 1 - k^2 \text{sech}^2(k(x - vt - s_0)),$$

it is clear that the continuous-wave background for the dark soliton (or the dimensionless chemical potential μ_0) is normalized by one, such that $\lim_{|x| \rightarrow \infty} |u_{\text{ds}}|^2 = 1$. When $k \rightarrow 1$ and $|v| \rightarrow 0$, the dark soliton approaches the limit of a standing topological soliton (called the black soliton). When $k \rightarrow 0$ and $|v| \rightarrow 1$, the dark soliton approaches the limit of a small-amplitude shallow soliton (which satisfies the KdV approximation [18]).

It should be noticed that, in physical terms, the choice $\mu_0 = 1$ actually sets the number of atoms N of the condensate. In the framework of the Thomas-Fermi approximation [27], it can be found that $N = (4\sqrt{2}/3)(\xi n_0/\Omega)\mu_0^{3/2}$, and, thus, for $n_0 \approx 10^8 \text{ m}^{-3}$, $\xi \sim 0.1$ – 1 microns (which are realistic value of the healing length for quasi-1D Rb BECs) and $\Omega \sim 10^{-2}$, the choice $\mu_0 = 1$ leads to a number of atoms of the order of $N \sim 10^3$ – 10^4 .

When $\epsilon \neq 0$, but the nonlinearity is crossed out by the linearization, the parabolic potential of the GP equation (2) has the ground state solution:

$$u_{\text{gs}}(x, t) = u_0 \exp\left(-\frac{\epsilon x^2 + i\epsilon t}{\sqrt{2}}\right), \quad (4)$$

where $u_0 \in \mathbb{C}$ is an arbitrary parameter of the ground state amplitude. When the nonlinear term of the defocusing GP equation (2) is taken into account, the linear mode (4) generates a family of ground state solutions by means of a standard local bifurcation [28],

$$u_{\text{gs}}(x, t) = U_\epsilon(x)e^{-i\mu_\epsilon t + i\theta_0}, \quad (5)$$

where $\mu_\epsilon \in \mathbb{R}$ is the normalized chemical potential and $\theta_0 \in \mathbb{R}$ is an arbitrary phase. Due to the scaling invariance of the GP equation (2), the amplitude of the ground state $U_\epsilon(x) \in \mathbb{R}$ can be uniquely normalized by one, such that $|U_\epsilon(0)|^2 = 1$.

The first excited state of the parabolic potential bifurcates from the linear solution:

$$u_{1es}(x, t) = x \exp\left(-\frac{\epsilon x^2 + 3i\epsilon t}{\sqrt{2}}\right), \quad (6)$$

by means of the same local bifurcation [28]. The first excited state corresponds to a static bound state between the dark soliton (3) placed at the center $x = 0$ of the nonlinear ground state (5). The solution for the static bound state exists for any $\epsilon \neq 0$ but tells nothing about dynamics of the dark soliton placed near the center of the ground state.

Dynamics of dark soliton is considered in this paper. We show that the dark soliton (3) undertakes adiabatic dynamics in the limit $\epsilon \rightarrow 0$, such that the parameter $(s_0 + vt) \equiv s(T)/\epsilon$ of position of the dark soliton (3) becomes a function of slow time $T = \epsilon t$, while the velocity parameter v is defined as $v(T) = \dot{s}$. The adiabatic dynamics leads to generation of radiative waves, which escape the dark soliton but become trapped by the parabolic potential. In the decomposition of the solution $u(x, t)$ into two (inner and outer) asymptotic scales, the leading-order radiative effects are taken into account when parameter $\theta_0 \equiv \theta(T)$ of complex phase of the dark soliton (3) depends also on $T = \epsilon t$ and the first-order corrections to the dark soliton (3) grow linearly in x . When reflections from the trapping potential are neglected, the extended dynamical equation for the position $s(T)$ of the dark soliton (3) takes the form:

$$\ddot{s} + s = \frac{\epsilon \dot{s}}{2\sqrt{(1-s^2)^3}\sqrt{1-s^2-\dot{s}^2}} + \mathcal{O}(\epsilon^2), \quad (7)$$

in the domain $(s, \dot{s}) \in \mathcal{D}_0$, where \mathcal{D}_0 is the unit disk:

$$\mathcal{D}_0 = \{(s, \dot{s}) \in \mathbb{R}^2 : s^2 + \dot{s}^2 < 1\}. \quad (8)$$

The left-hand-side of the dynamical equation (7) represents the leading-order adiabatic dynamics of the dark soliton oscillating on the ground state of the trapping potential. The right-hand-side represents the leading-order radiative effects (sound emission), when reflections of radiation from the parabolic potential are neglected. Within the truncation error of $\mathcal{O}(\epsilon^2)$, the ground state (5) can be approximated by the Thomas–Fermi (TF) approximation $U_\epsilon(x) = \sqrt{1 - \epsilon^2 x^2}$ on the scale $|x| < \epsilon^{-1}$.

The only equilibrium point of the dynamical equation (7) is $(0, 0)$ and it corresponds to the static bound state bifurcating from the first excited state (6). The leading-order part of the dynamical equation (7) describes a harmonic oscillator with the obvious solution: $s(T) = s_0 \cos(T + \delta_0)$. This result is well-known from earlier papers [8, 9, 10], where it was derived in the limit of black soliton, when $k \rightarrow 1$ and $|v| \rightarrow 0$. In the derivation presented herein, we have not used the assumption on the initial position $s(0)$ and speed $\dot{s}(0)$ of the dark soliton, and therefore, the approximation of the harmonic oscillator (7) remains valid for larger values of (s, \dot{s}) inside the unit disk (8).

We note that the velocity-dependent correction to the frequency of the harmonic oscillator (7) was obtained in an earlier study (see Eq. (36) in [10]), but it is not confirmed within our analysis. On the other hand, our results confirm the results of the shallow soliton approximation [18] which establishes the same frequency of oscillations as in the black soliton limit. In addition, the uniform frequency of oscillations for dark solitons of all amplitudes and velocities was recently reported by means of the energy (Hamiltonian) computations [17].

Let E be the energy of the harmonic oscillator:

$$E = \frac{1}{2}(\dot{s}^2 + s^2). \quad (9)$$

The energy increases in time due to the first-order correction terms of the main equation (7):

$$\dot{E} = \frac{\epsilon \dot{s}^2}{2\sqrt{(1-s^2)^3}\sqrt{1-s^2-\dot{s}^2}} + \mathcal{O}(\epsilon^2) > 0, \quad (10)$$

where $(s, \dot{s}) \in \mathcal{D}_0$. Due to the energy pumping (10), the amplitude of the harmonic oscillator increases in time. When the oscillation amplitude grows, the dark soliton (3) shifts from the black soliton limit $k \rightarrow 1$, $|v| \rightarrow 0$ to the shallow soliton limit $k \rightarrow 0$, $|v| \rightarrow 1$. By the Poincaré–Bendixon Theorem, the limit cycle does not exist in the unit disk (8) and all orbits approach the boundary of the disk, where the main equation (7) becomes invalid. The growth rate of the oscillation amplitude is nonlinear in general and depends on (s, \dot{s}) .

In the limit $s^2 + \dot{s}^2 \rightarrow 0$, the main equations (7) and (10) can be simplified. First, the energy of the dark soliton oscillations accelerates by the squared law $\dot{E} = \epsilon \dot{s}^2/2$, which is postulated in [19] and confirmed in numerical computations where the dark solitons oscillated in a tight dimple trap (see Fig. 2 in [19]). Second, the nonlinear equation (7) is linearized as follows:

$$\ddot{s} + s - \frac{\epsilon}{2}\dot{s} = \mathcal{O}(\epsilon^2, s^3),$$

which shows that the center point $(0, 0)$ becomes an unstable spiral point on the plane (s, \dot{s}) as $0 < \epsilon \ll 1$, with the leading-order solution: $s(T) = s_0 e^{\epsilon T/4} \cos(T + \delta_0)$. Therefore, due to radiative losses, the amplitude of oscillations of dark solitons increases while its own amplitude

decreases. This main result of the asymptotic analysis was also confirmed by numerical simulations where the dark solitons oscillated between two Gaussian humps (see Fig. 9 in [20]).

Figure 1 shows a spatio-temporal contour plot of the reduced density (the ground state density subtracted from the actual density) for a one-dimensional BEC confined in a parabolic trap with normalized strength $\epsilon = 0.05$ (the TF radius is equal to 20). The figures were obtained by numerical integration of the GP equation (2). The white areas correspond to a dark soliton, initially placed at the trap center (i.e., $s(0) = 0$) with an initial velocity $v(0) = 0.1$ (bottom panel) and $v(0) = 0.5$ (top panel). The plot is compared to the two versions of the main equation (7). The solid lines correspond to harmonic oscillations (within the adiabatic soliton dynamics), while the dashed ones correspond to the growing oscillations (within the inhomogeneity-induced sound emission). It is seen from the figures that the dashed lines approximate better the actual dark soliton motion within the first period of oscillations for $0 \leq t \leq t_* < T_{osc}$, where $T_{osc} = 2\pi/\epsilon$. For instance, a better agreement is achieved at the first turning points where, due to stronger sound emission, a slight increase of the amplitude of soliton oscillations is readily observed.

Nevertheless, for longer times, the anti-damped approximation of the main equation (7) becomes irrelevant due to the fact that the radiation cannot escape the trap and is reflected back to the dark soliton. As a result, the soliton continuously interacts with the reflected radiation so that, on average, the soliton reabsorbs the radiation it emits on the contrast to numerical computations in [19, 20]. We note that the sound emission is much weaker for the deeper soliton (with $v = 0.1$) and consequently the analytical result pertaining to the adiabatic approximation of the soliton motion is much closer to the result obtained by the numerical simulation.

The developed method allows us to incorporate multiple sound reflections and their recombination to the asymptotic equations for the dark soliton. If this is done, the main equation (7) is extended by an additional term due to multiple reflections beyond the initial time interval $0 \leq t \leq t_*$. This complication is however beyond the scopes of the present paper.

III. GROUND STATE OF THE GP EQUATION

We start with analysis of the ground state solution of the GP equation (2) in the form (5), where $(U_\epsilon(x), \mu_\epsilon)$ is a real-valued pair of eigenfunctions and eigenvalues of the nonlinear boundary-value problem:

$$\frac{1}{2}U'' - \epsilon^2 x^2 U - U^3 + \mu U = 0, \quad x \in \mathbb{R}^+, \quad (11)$$

subject to the normalized boundary conditions:

$$U_\epsilon(0) = 1, \quad U'_\epsilon(0) = 0, \quad \lim_{x \rightarrow \infty} U_\epsilon(x) = 0. \quad (12)$$

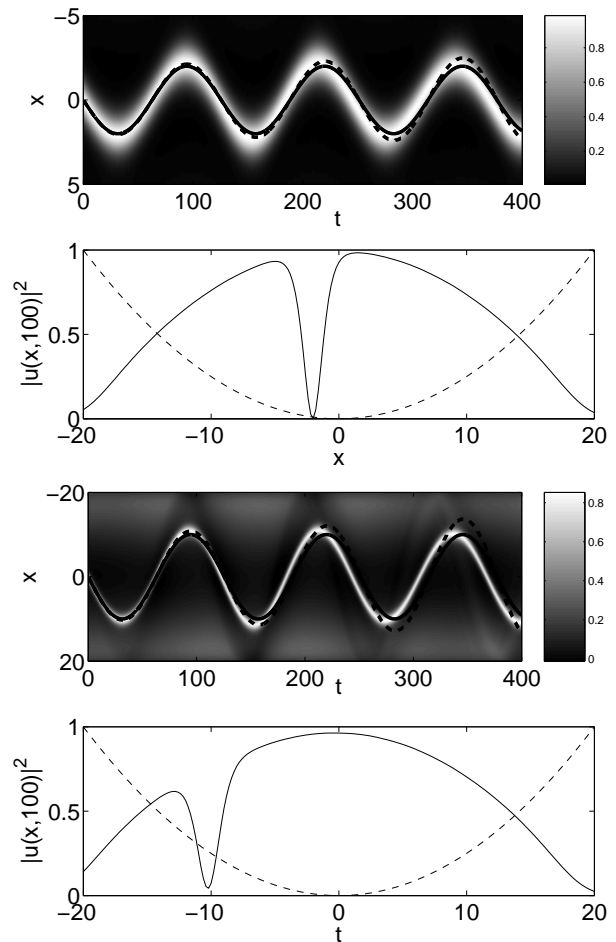


FIG. 1: Spatio-temporal evolution of the reduced condensate density (the ground state density minus the actual density) for the GP equation (2) with $\epsilon = 0.05$, $s(0) = 0$, and $v(0) = 0.1$ (top two panels), $v(0) = 0.5$ (bottom two panels). The solid lines correspond to the solutions of the harmonic (adiabatic) approximation and the dashed lines correspond to the anti-damped approximation (pertaining to sound emission). The dotted line on the plot of $|u(x,100)|^2$ shows the parabolic trapping potential.

We are interested in existence of the symmetric ground state $U_\epsilon(x) > 0$, $U_\epsilon(-x) = U_\epsilon(x)$ on $x \in \mathbb{R}$ for small values of ϵ^2 . We recall two facts for the boundary-value problem (11) with a given value of $\epsilon > 0$ (see [28]): (i) the local bifurcation from the linear ground state (4) occurs for $\mu > \mu_0(\epsilon)$, where $\mu_0 = \epsilon/\sqrt{2}$, and (ii) the nonlinear ground state (5) exists as a one-parameter smooth family, parameterized by μ or, equivalently, by $U(0)$. Moreover, $U(0)$ is an increasing function of $\mu > \mu_0(\epsilon)$ for a fixed value of ϵ . Therefore, for a given value of $\epsilon > 0$, there exists a unique value of μ (called μ_ϵ), which corresponds to the normalization $U_\epsilon(0) = 1$ and the solution pair $(U_\epsilon(x), \mu_\epsilon)$ is a smooth function of ϵ . The solution of the boundary-value problem of (11)–(12) can be approximated numerically by means of a contraction mapping method. Figure 2 shows the dependence of μ_ϵ versus ϵ ,

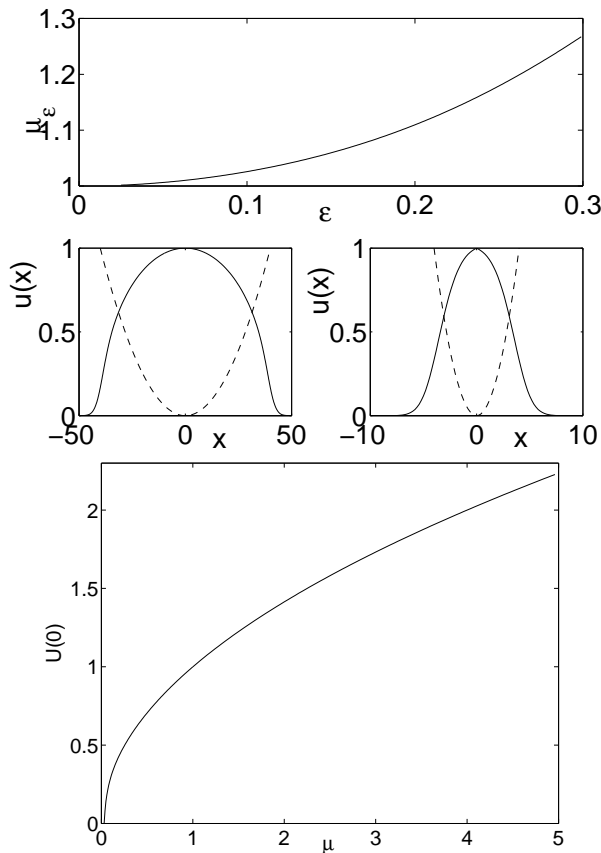


FIG. 2: Ground state solution of the boundary-value problem (11). Top panel: The dependence of μ_ϵ versus ϵ for fixed $U_\epsilon(0) = 1$. Middle panels: Profiles of the function $U(x)$ for two different values of the trap strength: $\epsilon = 0.025$ (left) and $\epsilon = 0.25$ (right). Bottom panel: The dependence of $U(0)$ versus μ for fixed $\epsilon = 0.05$.

the profile $U_\epsilon(x)$ for different values of ϵ , and the dependence of $U(0)$ versus μ , for fixed $\epsilon = 0.05$.

The solution of the ODE (11) with initial values $U(0) = 1$ and $U'(0) = 0$ can be constructed in the power series form:

$$U(x) = 1 + \sum_{k=1}^{\infty} a_k x^{2k}, \quad (13)$$

where coefficients $\{a_k\}_{k=1}^{\infty}$ can be found recursively, e.g. the first two terms are:

$$\begin{aligned} a_1 &= 1 - \mu, \\ a_2 &= \frac{1}{6} (\epsilon^2 + (1 - \mu)(3 - \mu)). \end{aligned}$$

The parameter $\mu = \mu_\epsilon$ is defined from the decay condition at infinity, where $U = U_\epsilon(x)$ and $\lim_{x \rightarrow \infty} U_\epsilon(x) = 0$. However, the decay condition is computationally inefficient for approximations of the dependence of μ_ϵ versus ϵ . A different (WKB) method was used for approximations of the solution $U_\epsilon(x)$ and the dependence μ_ϵ in [10, 18].

The advantage of the WKB method over the power series (13) is that the dependence μ_ϵ is determined from the condition at $x = 0$ rather than from the decay condition as $x \rightarrow \infty$.

In the WKB method, the solution of the ODE (11) is represented in the form $U(x) = \sqrt{Q(x)}$, where $Q(x)$ satisfies the equivalent problem:

$$Q(x) = \mu - \epsilon^2 x^2 + \frac{Q''(x)}{4Q(x)} - \frac{Q'^2(x)}{8Q^2(x)}. \quad (14)$$

In the limit of small ϵ , the solution of the ODE (14) can be thought in the form of a WKB asymptotic series:

$$Q = \mu - X^2 + \sum_{k=1}^{\infty} \epsilon^{2k} Q_k(X), \quad (15)$$

where $X = \epsilon x$, $|X| < \sqrt{\mu}$, and the set $\{Q_k(X)\}_{k=1}^{\infty}$ can be found recursively, e.g. the first two terms are:

$$Q_1 = -\frac{\mu}{2(\mu - X^2)^2}$$

and

$$Q_2 = \frac{Q_1'(X)}{4(\mu - X^2)} + \frac{XQ_1'(X) + Q_1(X)}{2(\mu - X^2)^2} + \frac{X^2Q_1(X)}{(\mu - X^2)^3}.$$

The symmetry in X implies that the condition $Q'(0) = 0$ is satisfied. The normalization condition $Q(0) = 1$ defines the power approximation of the dependence $\mu = \mu_\epsilon$ versus ϵ :

$$Q(0) = \mu - \frac{\epsilon^2}{2\mu} - \frac{3\epsilon^4}{4\mu^3} + O(\epsilon^6) = 1, \quad (16)$$

such that

$$\mu_\epsilon = 1 + \frac{\epsilon^2}{2} + \frac{\epsilon^4}{2} + O(\epsilon^6). \quad (17)$$

Using the leading-order approximation for μ_ϵ , we find an asymptotic approximation for $U_\epsilon(x)$ from the WKB asymptotic series (15):

$$U_\epsilon(x) = \sqrt{1 - \epsilon^2 x^2} + \epsilon^2 \tilde{U}(\epsilon x, \epsilon), \quad (18)$$

where $\tilde{U}(\epsilon x, \epsilon)$ is the remainder term. The leading-order approximation in (18) is referred to as the Thomas-Fermi approximation [27]. The WKB asymptotic series (15) gives a bounded approximation of the solution pair $(U_\epsilon(x), \mu_\epsilon)$ for $|\epsilon x| < \sqrt{\mu_\epsilon}$ but it becomes invalid at and beyond the turning points at $|\epsilon x| \geq \sqrt{\mu_\epsilon}$ [29]. Therefore, the Thomas-Fermi approximation (18) is valid only for $|\epsilon x| < 1$ in the limit of small ϵ .

IV. TRANSFORMATION OF THE GP EQUATION

We proceed with analysis of dynamics of the dark soliton on the ground state of the parabolic potential. This

problem can be studied after the equivalent transformation of the GP equation (2):

$$u(x, t) = U_\epsilon(x)w(x, t)e^{-i\mu_\epsilon t}, \quad (19)$$

where $(U_\epsilon(x), \mu_\epsilon)$ is the solution pair of the boundary-value problem (11)–(12) and $w(x, t)$ is a new variable. The function $w(x, t)$ satisfies the PDE problem:

$$iw_t + \frac{1}{2}w_{xx} + U_\epsilon^2(x)(1 - |w|^2)w = -\frac{U'_\epsilon(x)}{U_\epsilon(x)}w_x. \quad (20)$$

We will use the fact that $U_\epsilon(x) \equiv U_\epsilon(X)$, $X = \epsilon x$ in the asymptotic region $|\epsilon x| < 1$ as $\epsilon \rightarrow 0$. Assuming that the dynamics of the dark soliton occurs inside the asymptotic region $|\epsilon x| < 1$, we introduce the traveling wave coordinate for the dark soliton:

$$\eta = x - \frac{s(T)}{\epsilon}, \quad T = \epsilon t, \quad (21)$$

where the dependence $s(T)$ is to be determined, and expand the function $U_\epsilon(X)$ in the Taylor series near $X = s(T)$:

$$\begin{aligned} U_\epsilon(X) &= U_\epsilon(s(T) + \epsilon\eta) \\ &= U_\epsilon(s) + \epsilon\eta U'_\epsilon(s) + \frac{1}{2}\epsilon^2\eta^2 U''_\epsilon(s) + O((\epsilon\eta)^3). \end{aligned} \quad (22)$$

As a result, the PDE problem (20) takes the form of the perturbed equation:

$$\begin{aligned} iw_t - iw w_\eta + \frac{1}{2}w_{\eta\eta} + U_\epsilon^2(s)(1 - |w|^2)w \\ = -\epsilon \left(\frac{U'_\epsilon(s)}{U_\epsilon(s)}w_\eta + 2U_\epsilon(s)U'_\epsilon(s)\eta(1 - |w|^2)w \right) \\ - \epsilon^2 \frac{(U''_\epsilon(s)U_\epsilon(s) - U_\epsilon'^2(s))}{U_\epsilon^2(s)}\eta w_\eta \\ - \epsilon^2\eta^2 (U_\epsilon(s)U''_\epsilon(s) + U_\epsilon'^2(s)) (1 - |w|^2)w + O(\epsilon^3), \end{aligned}$$

where $v(T) = \dot{s}$ is the speed of the dark soliton. The perturbed equation is simplified with the scaling transformation:

$$z = \eta U_\epsilon(s(T)), \quad v(T) = \nu(T)U_\epsilon(s(T)), \quad (23)$$

such that the wave function $w(z, t)$ satisfies the perturbed defocusing NLS equation:

$$\begin{aligned} iw_t + U_\epsilon^2(s) \left[-i\nu w_z + \frac{1}{2}w_{zz} + (1 - |w|^2)w \right] \\ + R(w, \bar{w}) = 0, \end{aligned} \quad (24)$$

where $R = \epsilon R_1 + \epsilon^2 R_2 + O(\epsilon^3)$ are perturbation terms, with the first two of them being:

$$\begin{aligned} R_1 &= U'_\epsilon(s) (i\nu z w_z + w_z + 2z(1 - |w|^2)w) \\ R_2 &= \frac{(U''_\epsilon(s)U_\epsilon(s) - U_\epsilon'^2(s))}{U_\epsilon^2(s)} z w_z \\ &+ \frac{(U_\epsilon(s)U''_\epsilon(s) + U_\epsilon'^2(s))}{U_\epsilon^2(s)} z^2 (1 - |w|^2)w. \end{aligned}$$

Since $U_\epsilon(s) > 0$ for the ground state of the parabolic potential, the perturbation terms of the equation (24) are regular for any $s \in \mathbb{R}$. However, since the representation $U_\epsilon(x) \equiv U_\epsilon(X)$ is valid only for $|X| < 1$ in the limit of small ϵ , we consider the perturbed NLS equation (24) in the region where $|s| < 1$. The leading-order part of the defocusing NLS equation (24) (when $R(w, \bar{w}) = 0$) has the exact solution for the dark soliton:

$$w(z, t) = w_0(z) = \kappa \tanh(\kappa z) + i\nu, \quad (25)$$

where $\kappa = \sqrt{1 - \nu^2}$ and $\nu(T) = \nu_0$ is a constant speed. The time evolution of the dark soliton (25) in the case $R(w, \bar{w}) \neq 0$ is studied with a regular perturbation theory for dark solitons [12, 13, 14, 15].

V. ASYMPTOTIC MULTI-SCALE EXPANSION METHOD

The solution to the perturbed NLS equation (24) can be obtained in the form of an asymptotic multi-scale expansion series for the perturbed dark soliton (25) [13]:

$$w(z, t) = [w_0 + \epsilon w_1 + \epsilon^2 w_2 + O(\epsilon^3)] e^{i\theta}, \quad (26)$$

where $T = (\epsilon t, \epsilon^2 t, \dots)$, the function $w_0 = w_0(z; T)$ is the dark soliton (25), while the functions $w_1 = w_1(z, t; T)$ and $w_2 = w_2(z, t; T)$ solve the inhomogeneous linear problems:

$$\begin{aligned} i\partial_t \sigma_3 \mathbf{w}_1 + U_\epsilon^2(s) \mathcal{H} \mathbf{w}_1 = \dot{\theta} \mathbf{w}_0 - i\partial_T \sigma_3 \mathbf{w}_0 \\ - \mathbf{R}_1(w_0, \bar{w}_0) \end{aligned} \quad (27)$$

and

$$\begin{aligned} i\partial_t \sigma_3 \mathbf{w}_2 + U_\epsilon^2(s) \mathcal{H} \mathbf{w}_2 = \dot{\theta} \mathbf{w}_1 - i\partial_T \sigma_3 \mathbf{w}_1 \\ - \mathbf{N}_2(w_1, \bar{w}_1) - D\mathbf{R}_1(w_0, \bar{w}_0) \mathbf{w}_1 - \mathbf{R}_2(w_0, \bar{w}_0). \end{aligned} \quad (28)$$

Parameters $s(T)$ and $\theta(T)$ are to be determined from solutions of the inhomogeneous problems, while $\nu(T) = \dot{s}/U_\epsilon(s)$. In the problems (27) and (28), we have introduced the notations: \mathbf{w}_k and \mathbf{R}_k for vectors $(w_k, \bar{w}_k)^T$, $k = 0, 1, 2$ and $(R_k, \bar{R}_k)^T$, $k = 1, 2$, $D\mathbf{R}_1$ for the Jacobian of \mathbf{R}_1 , \mathbf{N}_2 for the quadratic terms from the left-hand-side of the unperturbed NLS equation. The self-adjoint linearization operator is

$$\mathcal{H} = -i\nu\sigma_3\partial_z + \sigma_0 \left(\frac{1}{2}\partial_z^2 + 1 \right) - \begin{pmatrix} 2|w_0|^2 & w_0^2 \\ \bar{w}_0^2 & 2|w_0|^2 \end{pmatrix}.$$

where $\sigma_0 = \text{diag}(1, 1)$ and $\sigma_3 = \text{diag}(1, -1)$. Analysis of the first-order problem (27) predicts a leading-order equation for $s(T)$, which characterizes oscillations of dark solitons near the center of the parabolic potential. The first-order problem also describes the leading-order radiation from the dark soliton to infinity, related to the equation for $\theta(T)$. Analysis of the second-order problem (28) predicts a first-order correction to the equation for $s(T)$,

which is induced by the leading-order radiation. Due to radiation, the oscillation amplitude grows in time so that the amplitude of the dark soliton decreases. Derivation of all these results is divided into several technical subsections.

A. Linearization operator

The self-adjoint operator \mathcal{H} is defined on complete Hilbert space $H^1(\mathbb{R}, \mathbb{C}^2) \subset L^2(\mathbb{R}, \mathbb{C}^2)$. It has a non-empty kernel:

$$\mathcal{H}\mathbf{w}'_0(z) = \mathbf{0}, \quad (29)$$

which is related to translational invariance of the unperturbed NLS equation in z . Furthermore, the operator \mathcal{H} has two branches of the continuous spectrum:

$$\sigma_{\text{ess}}(\mathcal{H}) = (-\infty, -2] \cup (-\infty, 0], \quad (30)$$

such that the second branch intersects the kernel. The only bounded non-decaying eigenvector for the zero eigenvalue, which belongs to the continuous spectrum (30), is related to the gauge invariance of the NLS equation:

$$\mathcal{H}(i\sigma_3\mathbf{w}_0) = \mathbf{0}. \quad (31)$$

The homogeneous equation $\mathcal{H}\mathbf{w} = \mathbf{0}$ supports the decaying solution (29), the bounded solution (31), a linearly growing solution, and an exponentially growing solution. The linearly growing solution can be found explicitly [13]:

$$\mathcal{H}\left(i\sigma_3 z\mathbf{w}_0 - \partial_\nu\mathbf{w}_0 + \frac{3\nu}{2\kappa}\partial_\kappa\mathbf{w}_0\right) = \mathbf{0}. \quad (32)$$

Here and henceforth, it is convenient to consider $w_0(z)$ as a function of two independent parameters κ and ν . The relation $\kappa = \sqrt{1 - \nu^2}$ is used after evaluating the partial derivatives of $w_0(z)$ in κ and ν .

The linearization operator $\sigma_3\mathcal{H}$ has the kernel (29) and the generalized kernel:

$$\sigma_3\mathcal{H}\left(\partial_\nu\mathbf{w}_0 - \frac{\nu}{\kappa}\partial_\kappa\mathbf{w}_0\right) = i\mathbf{w}'_0(z). \quad (33)$$

The spectrum of $\sigma_3\mathcal{H}$ includes two branches of the continuous spectrum:

$$\sigma_{\text{ess}}(\sigma_3\mathcal{H}) = \mathbb{R} \cup \mathbb{R}. \quad (34)$$

The spectrum of $\sigma_3\mathcal{H}$ consisting of the kernel (29), the generalized kernel (33) and the two branches of the continuous spectrum (34) is complete in $H^1(\mathbb{R}, \mathbb{C}^2)$ [14, 15]. Nevertheless, since the kernel of \mathcal{H} has also a bounded non-decaying eigenvector (31), we construct a bounded non-decaying eigenvector from the nonhomogeneous problem:

$$\sigma_3\mathcal{H}\left(\frac{1}{2\kappa}\partial_\kappa\mathbf{w}_0\right) = i(i\sigma_3\mathbf{w}_0). \quad (35)$$

The eigenvectors (31) and (35) are not in $L^2(\mathbb{R}, \mathbb{C}^2)$. This fact implies (see [13]) that adiabatic dynamics of the dark soliton (the decaying component) induces radiative waves of the continuous spectrum (the bounded non-decaying component) already at the first order of the perturbation theory. The coupling between the decaying and non-decaying components is computed from the dynamical equations on parameters $s(T)$ and $\theta(T)$.

B. The leading-order frequency of oscillations

The linear inhomogeneous problem (27) leads to a secular growth of $w_1(z, t; T)$ in t unless the right-hand-side is orthogonal to the kernel of \mathcal{H} . The orthogonality condition defines a nonlinear equation on parameters of the dark soliton (25):

$$\begin{aligned} & \frac{1}{2} \int_{-\infty}^{\infty} \text{sech}^2(\kappa z) \text{Im}(\partial_T w_0) d(\kappa z) \\ &= \frac{1}{2} \int_{-\infty}^{\infty} \text{sech}^2(\kappa z) \text{Re}(R_1(w_0, \bar{w}_0)) d(\kappa z). \end{aligned} \quad (36)$$

By computing the integrals directly, we obtain the system of dynamical equations:

$$\dot{\nu} = (1 - \nu^2)U'_\epsilon(s), \quad \dot{s} = \nu U_\epsilon(s), \quad (37)$$

where the last equation is due to the relation (23) between $\nu(T)$ and $v(T) = \dot{s}$. Closing the system of dynamical equations, we find the governing equation for the position of the dark soliton:

$$\ddot{s} + V'(s) = 0, \quad V(s) = \frac{1}{2}(1 - U_\epsilon^2(s)). \quad (38)$$

The governing equation (38) is equivalent to the Hamiltonian system of a particle moving in a potential field, where $V(s)$ stands for the effective potential energy of the particle.

Using the WKB asymptotic series (15) for $U_\epsilon^2(x)$ and the power approximation (17) for μ_ϵ , we find the power approximation for the potential function $V(s)$:

$$V(s) = \frac{s^2}{2} + \frac{\epsilon^2 s^2 (2 - s^2)}{4(1 - s^2)^2} + \mathcal{O}(\epsilon^4), \quad (39)$$

where $|s| < 1$. Since the system (38) is valid at the leading order of the asymptotic series, the dark soliton oscillates as a harmonic oscillator in the limit $\epsilon \rightarrow 0$:

$$\ddot{s} + s = 0, \quad (40)$$

which is equivalent to the left-hand-side of the main equation (7). The equation (40) for harmonic oscillator is valid in the unit disk (8). Since the solutions $s(T) = s_0 \cos(T + \delta_0)$ represent circles of radius s_0 on the phase plane (s, \dot{s}) , the trajectories remain inside the disk (8) whenever $s_0 < 1$.

We note that the $O(\epsilon^2)$ corrections of the power approximation (39) are beyond the Tomas-Fermi approximation (18). These terms can be dropped in the main equation (38), since the $O(\epsilon)$ corrections to the main equation (38) occur from the solution of the second-order inhomogeneous equation (28).

C. The first-order radiation corrections

After the constraint (36) is added, the linear inhomogeneous equation (27) can be solved for $w_1(z, t; T)$, such that $w_1(z, t; T)$ is bounded in t . We adopt a standard assumption of the asymptotic multi-scale expansion method that the solution $w_1(z, t; T)$ approaches the stationary solution $w_{1s}(z; T)$ as $t \rightarrow \infty$ due to dispersive decay estimates. The stationary solution $w_{1s}(z; T)$ can be represented in the form:

$$w_{1s} = \frac{q(T)}{U_\epsilon^2(s)} (izw_0 - \partial_\nu w_0) + \frac{3\nu q(T) - \dot{\theta}(T)}{2\kappa U_\epsilon^2(s)} \partial_\kappa w_0 + \tilde{w}_{1s}(z; T). \quad (41)$$

The first two terms in (41) represent the linearly growing (32) and bounded (35) eigenvectors. The last term $\tilde{w}_{1s}(z; T)$ is a t -independent solution of the inhomogeneous equation (27) which corresponds to the last two terms in the right-hand-side of (27) under the constraint (37). We do not include the decaying (29) and bounded (31) solutions of the kernel of \mathcal{H} in the representation (41) as they renormalize parameters $\theta(T)$ and $s(T)$.

The dependence of $q(T)$ and $\dot{\theta}(T)$ is defined from the radiation problem, associated to the behavior of the stationary solution $w_{1s}(z; T)$ as $|z| \rightarrow \infty$. Let $w_{1s}^\pm(z; T)$ represent a linearly growing solution $w_{1s}(z; T)$ as $z \rightarrow \pm\infty$. Neglecting exponentially small terms in the limits $z \rightarrow \pm\infty$, we obtain from (27) the linear inhomogeneous problem for $w_{1s}^\pm(z; T)$:

$$U_\epsilon^2(s) \left[\frac{1}{2} w_{1s}^{\pm\prime\prime} - i\nu w_{1s}^{\pm\prime} - w_{1s}^\pm - (\kappa \pm i\nu)^2 \bar{w}_{1s}^\pm \right] = \dot{\theta}(i\nu \pm \kappa) + \frac{\dot{\nu}}{\kappa} (\kappa \pm i\nu). \quad (42)$$

The most general linearly growing solution of the inhomogeneous equation (42) has the form:

$$w_{1s}^\pm = \frac{1}{U_\epsilon^2(s)} [(a_1 \pm b_1)iz(\pm\kappa + i\nu) + (a_2 \pm b_2)], \quad (43)$$

where $a_{1,2}$ and $b_{1,2}$ satisfy two relations:

$$\nu a_1 - 2\kappa b_2 = \dot{\theta}, \quad \nu b_1 - 2\kappa a_2 = \frac{\dot{\nu}}{\kappa}. \quad (44)$$

The first two terms in the solution (41) have odd real parts and even imaginary parts in z , while the component $\tilde{w}_{1s}(z, T)$ has the opposite symmetry in z . Matching the

linear growing terms in (41) and (43) under the relation (44), we obtain that

$$a_1 = q, \quad b_2 = \frac{\nu q - \dot{\theta}}{2\kappa}. \quad (45)$$

We note that the constant terms in (41) and (43) are equivalent to the second equation (45) under the renormalization of $\theta = \theta_0^\pm + \epsilon\theta_1^\pm + O(\epsilon^2)$, where $\theta_1^\pm = \pm q/\kappa$. One more equation is needed for finding of values of a_2 and b_1 . This equation can be derived from the balance equation for the renormalized power of the perturbed NLS equation (24):

$$(\partial_t - \nu U_\epsilon^2(s)\partial_z) n(w, \bar{w}) + U_\epsilon^2(s)\partial_z j(w, \bar{w}) = l(w, \bar{w}),$$

where

$$\begin{aligned} n &= |w|^2 - 1, \\ j &= \frac{1}{2i} (\bar{w}w_z - \bar{w}_z w), \\ l &= i (\bar{w}R(w, \bar{w}) - w\bar{R}(w, \bar{w})). \end{aligned} \quad (46)$$

Computing explicitly the integral quantities and the jump conditions:

$$\begin{aligned} N &= \int_{-\infty}^{\infty} n(w, \bar{w}) dz = -2\kappa + O(\epsilon), \\ L &= \int_{-\infty}^{\infty} l(w, \bar{w}) dz = 2\nu\kappa U_\epsilon'(s)\epsilon + O(\epsilon^2) \end{aligned}$$

and

$$\begin{aligned} U_\epsilon^2(s) [n(w, \bar{w})]_-^+ &= 4\kappa a_2 \epsilon + O(\epsilon^2), \\ U_\epsilon^2(s) [j(w, \bar{w})]_-^+ &= 2b_1 \epsilon + O(\epsilon^2), \end{aligned}$$

we find another relation on a_2 and b_1 :

$$\kappa b_1 - 2\kappa^2 \nu a_2 = \nu\kappa^2 U_\epsilon'(s) - \nu\dot{\nu}. \quad (47)$$

Using the leading-order equation (37) for $\dot{\nu}$, we obtain that

$$b_1 = 2\kappa\nu a_2 = -\frac{\nu}{\kappa} U_\epsilon'(s). \quad (48)$$

Once the parameters a_1 , a_2 , b_1 , and b_2 in the asymptotic representation (43) are uniquely found, the stationary solution $w_s(z; T)$ can be defined outside the dark soliton up to the order of $O(\epsilon^2)$ terms:

$$\begin{aligned} \lim_{z \rightarrow \pm\infty} w_s(z, T) &= (1 + \epsilon W^\pm(X, T)) e^{i\Theta^\pm(X, T)} \\ &= [(\pm\kappa + i\nu) + \epsilon w_{1s}^\pm(z; T) + O(\epsilon^2)] e^{i(\theta_0^\pm + \epsilon\theta_1^\pm + O(\epsilon^2))}, \end{aligned}$$

where $X = \epsilon x$, $\epsilon z = U_\epsilon(s(T))(X - s(T))$,

$$\begin{aligned} W^\pm &= \frac{\kappa(b_2 \pm a_2)}{U_\epsilon^2(s)} + O(\epsilon), \\ \Theta^\pm &= \Theta_0^\pm(T) + \epsilon\Theta_1^\pm(T) + \epsilon z \frac{(a_1 \pm b_1)}{U_\epsilon^2(s)} + O(\epsilon^2), \end{aligned}$$

and the explicit forms for Θ_0^\pm and Θ_1^\pm are not written. The radiation fields $W^\pm(X, T)$ and $\Theta^\pm(X, T)$ are defined outside the dark soliton for $X \gtrless s(T)$, respectively, subject to the boundary conditions:

$$\begin{aligned} W^\pm \Big|_{X=s(T)} &= \frac{\kappa(b_2 \pm a_2)}{U_\epsilon^2(s)} + O(\epsilon), \\ \frac{\partial \Theta}{\partial X} \Big|_{X=s(T)} &= \frac{(a_1 \pm b_1)}{U_\epsilon(s)} + O(\epsilon). \end{aligned} \quad (49)$$

These conditions match the inner asymptotic expansion for $z = O(1)$ and the outer asymptotic expansion for $X = O(1)$ in the stationary solution $w_s(z; T)$ (see [13]).

D. Radiation problem for small-amplitude waves

We now consider the small-amplitude waves within the original equation (20) for $w(x, t)$. Using the polar form, $w(x, t) = R(x, t) \exp(i\Phi(x, t))$, we obtain the system:

$$\begin{aligned} R_t + R_x \Phi_x + \frac{1}{2} R \Phi_{xx} &= -\frac{U'_\epsilon(x)}{U_\epsilon(x)} R \Phi_x, \\ \Phi_t + \frac{1}{2} \Phi_x^2 - \frac{R_{xx}}{2R} - U_\epsilon^2(x)(1 - R^2) &= \frac{U'_\epsilon(x)}{U_\epsilon(x)} \frac{R_x}{R}. \end{aligned}$$

The small-amplitude long-wave solutions of the above system can be constructed in the asymptotic form:

$$\begin{aligned} R &= 1 + \epsilon W(X, T) + O(\epsilon^2), \\ \Phi &= \Theta(X, T) + O(\epsilon), \end{aligned}$$

where $X = \epsilon x$, $T = \epsilon t$ and we use the fact that $U_\epsilon(x) \equiv U_\epsilon(X)$ in the asymptotic region $|\epsilon x| < 1$ as $\epsilon \rightarrow 0$. The leading-order terms $W(X, T)$ and $\Theta(X, T)$ solve the coupled problem:

$$W_T + (U_\epsilon(X)V)_X + 2U'_\epsilon(X)V = 0, \quad (50)$$

$$(U_\epsilon(X)V)_T + (U_\epsilon^2(X)W)_X = 0, \quad (51)$$

where

$$V = \frac{\Theta_X}{2U_\epsilon(X)}. \quad (52)$$

Equivalently, the coupled problem (50)–(51) with the correspondence (52) reduces to the wave equation with a space-dependent speed:

$$\Theta_{TT} - (U_\epsilon^2(X)\Theta_X)_X = 0, \quad (53)$$

where

$$W = -\frac{\Theta_T}{2U_\epsilon^2(X)}. \quad (54)$$

The system (50)–(51) and the scalar equation (53) are to be solved separately for $X > s(T)$ and $X < s(T)$ subject to the boundary conditions (49). In addition,

two radiation boundary conditions must be added to the system (50)–(51) for a unique solution. Since the small-amplitude waves move faster than the dark soliton (indeed, $\dot{s}^2 < U_\epsilon^2(s) = 1 - s^2$ in the domain (8)), the radiative waves include the right-travelling wave for $X > s(T)$ and the left-travelling wave for $X < s(T)$. Figure 3 shows the upper-half (X, T) -plane, which is divided by the curve $X = s(T)$ into two domains D_r and D_l .

The wave equation (53) has two characteristics, which are defined by the principal part of the PDE system (50)–(51). Let $X = \xi_\pm(T)$ be the equations for the two characteristics curves, starting from a particular point $(s(\tau_0), \tau_0)$, where $\tau_0 > 0$. According to the standard text on PDEs [30], we find that the functions $\xi_\pm(T; \tau_0)$ solve the initial-value problem for $T \geq \tau_0$:

$$\frac{d\xi_\pm}{dT} = \pm U_\epsilon(\xi), \quad \xi_\pm(\tau_0; \tau_0) = s(\tau_0). \quad (55)$$

The components $R_\pm = W \pm V = R_\pm(T; \tau_0)$, defined along the characteristics $X = \xi_\pm(T; \tau_0)$, solve the system of evolution equations:

$$\frac{dR_+}{dT} = -\frac{1}{2} U'_\epsilon(\xi_+(T; \tau_0)) (5R_+ - R_-), \quad (56)$$

$$\frac{dR_-}{dT} = -\frac{1}{2} U'_\epsilon(\xi_-(T; \tau_0)) (R_+ - 5R_-). \quad (57)$$

Integrating the initial-value problem (55) in the Thomas-Fermi approximation $U_\epsilon(X) = \sqrt{1 - X^2}$, we find the explicit solution:

$$\xi_\pm(T; \tau_0) = \sin(\xi_0 \pm (T - \tau_0)), \quad (58)$$

where $\xi_0 = \arcsin(s(\tau_0))$. The families of two characteristics intersect transversely the dark soliton curve $X = s(T)$ at any point $(s(\tau_0), \tau_0)$ (see Figure 3), where the components R_\pm are generated by means of the boundary conditions (49) and the radiation boundary conditions, which need to be added to the system (56)–(57).

Let us consider the domain D_r to the right of the curve $X = s(T)$. By geometry of the initial-value problem (see Figure 3) or by the symmetry of the coupled problem (56)–(57), the characteristics $\xi_-(T; \tau_1)$ and the component $R_-(T; \tau_1)$ in D_r are the same as the characteristics $\xi_+(T; \tau_0)$ and the component $R_+(T; \tau_0)$ in D_r . When integrating the evolution equation for $R_+(T; \tau_0)$, one needs to substitute the value for R_- , from its value on the transversally intersecting characteristics in D_r . Figure 3 shows two intersections of $\xi_+(T; \tau_0)$ for $\tau_0 < T < \tau_1$ with the characteristics to the point $(s(\tau), \tau)$. Before the reflection, $\xi_+(T; \tau_0)$ intersects with $\xi_-(T; \tau)$, such that $R_- = R_-(T; \tau)$. After the reflection, $\xi_+(T; \tau_0)$ intersects with $\xi_+(T; \tau)$, such that $R_- = R_+(T; \tau)$. At $T = \tau_1$, the matching formula gives a required radiation boundary condition:

$$R_-(\tau_1; \tau_1) = R_+(\tau_1, \tau_0). \quad (59)$$

The initial data for $R_+(\tau_0, \tau_0)$ are uniquely defined from (49) and (59).

Similarly, in the domain D_1 , we obtain the radiation boundary condition:

$$R_+(\tau_1; \tau_1) = R_-(\tau_1, \tau_0). \quad (60)$$

If no incoming waves are imposed initially for $T \leq 0$, then we obtain that $R_- = 0$ in D_r and $R_+ = 0$ in D_1 at least for $0 \leq T \leq \tau_*$, where τ_* is the first intersection of $\xi_+(T; 0)$ with $s(T)$, such that $\xi(\tau_*; 0) = s(\tau_*)$. Therefore, the components $V^\pm(X, T)$ and $W^\pm(X, T)$ of the radiative waves to the right and left of the dark soliton $X = s(T)$ are related at the moving boundary $X = s(T)$ by the radiation boundary conditions:

$$V^\pm \Big|_{X=s(T)} = \pm W^\pm \Big|_{X=s(T)}. \quad (61)$$

The latter conditions result by virtue of (49) and (52) in the constraints:

$$a_1 = 2\kappa a_2, \quad b_1 = 2\kappa b_2. \quad (62)$$

Using explicit formulas (45) and (48), we find unique expressions for $q(T)$ and $\dot{\theta}(T)$:

$$q = -\frac{U'_\epsilon(s)}{\kappa}, \quad \dot{\theta} = 0. \quad (63)$$

Relations (61)–(63) are valid within the first period of oscillations $0 \leq T \leq \tau_* < 2\pi$ under the condition that no incoming waves are generated initially. If absorbing boundary conditions for radiative waves are specified on the boundary of the TF radius ($X \approx \pm 1$), the relations (61)–(63) are extended for later times $T > \tau_*$. Otherwise, additional terms occur in the relations (61)–(63) due to multiple reflections, and these terms are defined by the solution of the coupled evolution problem (56)–(57) along characteristics (58) with the radiation boundary conditions (59)–(60).

E. The first-order corrections to the main equation

Radiative corrections to the main equation for $s(T)$ are derived from the second-order inhomogeneous equation (28) by means of the same orthogonality condition (36). Equivalently, radiative corrections can be computed from the balance equation for the renormalized momentum [13]:

$$\begin{aligned} (\partial_t - \nu U_\epsilon^2(s) \partial_z) p(w, \bar{w}) + U_\epsilon^2(s) \partial_z r(w, \bar{w}) \\ = \partial_z m(w, \bar{w}) + k(w, \bar{w}), \end{aligned} \quad (64)$$

where

$$\begin{aligned} p &= \frac{i}{2} (\bar{w} w_z - w \bar{w}_z) \left(1 - \frac{1}{|w|^2} \right), \\ r &= \frac{1}{4} (\bar{w} w_{zz} - 2\bar{w}_z w_z + w \bar{w}_{zz}) \left(1 - \frac{1}{|w|^2} \right) \\ &\quad - \frac{|w_z|^2}{2|w|^2} - \frac{1}{2} (1 - |w|^2)^2 \end{aligned}$$

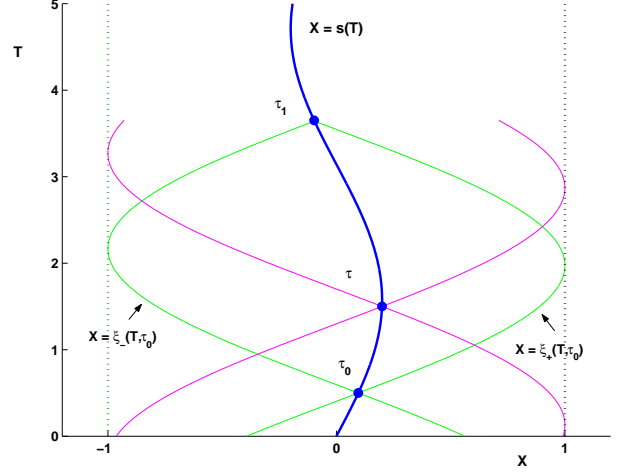


FIG. 3: The domain of the PDE system (50)–(51) and the family of two characteristics, superposed with the dark soliton curve $X = s(T)$.

and

$$\begin{aligned} m &= -\frac{1}{2} (\bar{w} R(w, \bar{w}) + w \bar{R}(w, \bar{w})) \left(1 - \frac{1}{|w|^2} \right), \\ k &= \bar{w}_z R(w, \bar{w}) + w_z \bar{R}(w, \bar{w}). \end{aligned}$$

Expanding the integral quantities and the jump conditions into the asymptotic approximations:

$$\begin{aligned} P &= \int_{-\infty}^{\infty} p(w, \bar{w}) dz = P_0 + \epsilon P_1 + O(\epsilon^2), \\ K &= \int_{-\infty}^{\infty} k(w, \bar{w}) dz = \epsilon K_1 + \epsilon^2 K_2 + O(\epsilon^3) \end{aligned}$$

and

$$\begin{aligned} U_\epsilon^4(s)[p]^\pm &= -4\epsilon^2 \kappa (a_1 a_2 + b_1 b_2) + O(\epsilon^3), \\ U_\epsilon^4(s)[r]^\pm &= -2\epsilon^2 (a_1 b_1 + 4\kappa^2 a_2 b_2) + O(\epsilon^3) \\ U_\epsilon^4(s)[m]^\pm &= O(\epsilon^3), \end{aligned}$$

we find the explicit expressions

$$\begin{aligned} P_0 &= 2\nu\kappa - 2 \arctan\left(\frac{\kappa}{\nu}\right), \\ U_\epsilon^2(s)P_1 &= 2\kappa q - q \partial_\nu P_0 + \frac{3\nu q - \dot{\theta}}{2\kappa} \partial_\kappa P_0 = 2U'_\epsilon(s), \\ K_1 &= 4\kappa(1 - \nu^2)U'_\epsilon(s), \\ U_\epsilon^2(s)K_2 &= -8\nu\kappa q U'_\epsilon(s) - q \partial_\nu K_1 + \frac{3\nu q - \dot{\theta}}{2\kappa} \partial_\kappa K_1 \\ &= -6\nu(U'_\epsilon(s))^2 \end{aligned}$$

and

$$U_\epsilon^4(s)[- \nu p + r]^\pm = -2\epsilon^2 \nu (U'_\epsilon(s))^2 + O(\epsilon^3).$$

We note that the expressions for P_0 and K_1 are found by using $w_0(z)$ in Eq. (25) as a function of two independent

parameters κ and ν . This technical trick allows us to compute the correction terms P_1 and K_2 by using partial derivatives of P_0 and K_1 in κ and ν . The final expressions use the relation $\kappa = \sqrt{1 - \nu^2}$ as well as the previously found relations (45), (48), and (63).

Substituting all expansions into the balance equation (64) and integrating on $z \in \mathbb{R}$, we obtain an extended main equation in the form:

$$\dot{\nu} - \kappa^2 U'_\epsilon(s) + \frac{\epsilon \nu U''_\epsilon(s)}{2\kappa U_\epsilon(s)} = \mathcal{O}(\epsilon^2).$$

Using the relation $\dot{s} = \nu U_\epsilon(s)$, the main equation can be rewritten for $s(T)$:

$$\ddot{s} - U_\epsilon(s) U'_\epsilon(s) + \frac{\epsilon \dot{s} U''_\epsilon(s)}{2\kappa U_\epsilon(s)} = \mathcal{O}(\epsilon^2). \quad (65)$$

Furthermore, using the Tomas-Fermi approximation $U_\epsilon(s) = \sqrt{1 - s^2}$, the extended dynamical equation is rewritten in the final form:

$$\ddot{s} + s = \frac{\epsilon \dot{s}}{2\kappa(1 - s^2)^2} + \mathcal{O}(\epsilon^2), \quad (66)$$

where

$$\kappa = \sqrt{\frac{1 - s^2 - \dot{s}^2}{1 - s^2}}$$

and $s^2 + \dot{s}^2 < 1$. We note that the perturbation term R_2 in the right-hand-side of the second-order problem (28) does not contribute to the main equation (66), since all associated integrals in the correction term K_2 are zero due to symmetry in $z \in \mathbb{R}$.

Second-order corrections $\mathcal{O}(\epsilon^2)$ to the extended equation (66) can be incorporated to the asymptotic theory if the second-order problem (28) is solved explicitly and the third-order problem associated to the perturbed NLS equation (24) is analyzed. It is beyond the scope of our manuscript to derive the error bounds between the solution of the perturbed NLS equation (24) and the truncated stationary solution of the first-order and second-order problems (27) and (28).

VI. FAILURE OF THE FORMAL PERTURBATION THEORY

We shall consider the perturbed GP equation in the form (20), where the ground state $U_\epsilon(x)$ is truncated by the Thomas-Fermi approximation (18), such that $U_\epsilon = \sqrt{1 - \epsilon^2 x^2}$. The perturbed GP equation (20) takes the explicit form:

$$i w_t + \frac{1}{2} w_{xx} + (1 - |w|^2) w = R(w, \bar{w}), \quad (67)$$

where

$$R(w, \bar{w}) = \epsilon^2 x^2 (1 - |w|^2) w + \frac{\epsilon^2 x}{1 - \epsilon^2 x^2} w_x.$$

The GP equation (67) has the exact solution for $R(w, \bar{w}) = 0$:

$$w(x, t) = w_0(\eta) = k \tanh(k\eta) + iv, \quad (68)$$

where

$$\eta = x - \frac{s(T)}{\epsilon}, \quad v(T) = \dot{s}, \quad T = \epsilon t. \quad (69)$$

If $w_0(\eta)$ is a steadily traveling dark soliton, parameters are constant, where $k = \sqrt{1 - v^2}$ is the amplitude and v is the speed. We assume that the coordinate $s(T)$ of the dark soliton changes adiabatically under the small perturbation $R(w, \bar{w}) \neq 0$ and show that a formal perturbation theory fails to capture the correct dependence of the frequency of oscillations. Using the same renormalized momentum equation (64), we obtain from (67) the leading-order balance equation for the renormalized momentum of the dark soliton [12, 14, 16]:

$$\epsilon \frac{dP_s}{dT} = - \int_{-\infty}^{\infty} w'_0(x) (R + \bar{R}) (w_0, \bar{w}_0) dx, \quad (70)$$

where

$$\begin{aligned} P_s &= \frac{i}{2} \int_{-\infty}^{\infty} (\bar{w}_0 w'_0 - w \bar{w}'_0) \left(1 - \frac{1}{|w_0|^2}\right) dx \\ &= 2vk - 2\arctan\left(\frac{k}{v}\right), \end{aligned} \quad (71)$$

such that

$$\epsilon \frac{dP_s}{dT} = - \frac{4\epsilon k^2 \dot{k}}{\sqrt{1 - k^2}}.$$

The same equation occurs in the Lagrangian averaging technique applied to the perturbed GP equation (67) (see [25] and references therein). The integrals in the right-hand-side of (70) can be evaluated at the leading-order approximation as $\epsilon \rightarrow 0$, when the scaling (69) is used. As a result, we have

$$\begin{aligned} \epsilon^2 \int_{-\infty}^{\infty} x^2 (1 - |w_0|^2) (|w_0|^2)' dx &= \frac{4}{3} \epsilon k^3 s + \mathcal{O}(\epsilon^3), \\ 2\epsilon^2 \int_{-\infty}^{\infty} \frac{x |w'_0|^2}{1 - \epsilon^2 x^2} dx &= \frac{8}{3} \frac{\epsilon k^3 s}{1 - s^2} + \mathcal{O}(\epsilon^3). \end{aligned}$$

Using the leading-order approximation $\dot{s} = \sqrt{1 - k^2}$, we close the main equation for $s(T)$ as follows:

$$\ddot{s} + \frac{(3 - s^2)(1 - \dot{s}^2)}{3(1 - s^2)} s = \mathcal{O}(\epsilon^2). \quad (72)$$

The main equation (72) represents the adiabatic approximation for dynamics of dark solitons, in neglecting of the radiative effects (see [16, 25]). In the limit of black soliton, when s is small, the equation for an anharmonic oscillator (72) approaches the equation for a harmonic oscillator (40). However, for a dark soliton of arbitrary amplitude, the anharmonic oscillator equation (72) is different from the harmonic oscillator equation (40), although

it represents the same asymptotic limit of adiabatic oscillations of the dark soliton.

The paradox above has a simple resolution. The first term in the right-hand-side of the perturbed GP equation (67) is not a small perturbation for the dark soliton (68) under the scaling (69) in the limit $\epsilon \rightarrow 0$. Indeed, $\epsilon^2 x^2 = s^2 - 2\epsilon s \eta + \epsilon^2 \eta^2$, such that the correct perturbed GP equation in the variables (69) takes the form:

$$i w_t - i v w_\eta + \frac{1}{2} w_{\eta\eta} + (1 - s^2)(1 - |w|^2)w = \tilde{R}(w, \bar{w}), \quad (73)$$

where

$$\tilde{R} = -2\epsilon s \eta(1 - |w|^2)w + \frac{\epsilon s}{1 - s^2} w_\eta + \mathcal{O}(\epsilon^2).$$

However, the dark soliton $w = w_0(\eta)$ is no longer a solution of the left-hand-side of the GP equation (73) and the renormalization of the variable η is required before formal application of the perturbation theory. The renormalization of the GP equation is developed in the main part of this paper. We conclude that the formal application of the perturbation theory to the perturbed GP equation (67) fails to recover an accurate dependence of frequency of dark soliton oscillations from the amplitude of the dark soliton.

VII. CONCLUSIONS

In this paper, we have analyzed the oscillations of dark solitons in trapped atomic Bose-Einstein condensates. We have considered a repulsive quasi-one-dimensional condensate, described by a Gross-Pitaevskii equation with a parabolic external trapping potential. An asymptotic multi-scale expansion method has been developed in the limit of the weakly trapped condensate. To the leading-order of approximation (i.e., neglecting the inhomogeneity-induced sound emission by the soliton),

the soliton motion is harmonic, with a constant frequency depending on the trap strength. This result bridges earlier predictions obtained by different approaches in two limiting cases, namely the adiabatic perturbation theory for nearly black solitons [9] and the Korteweg-deVries approximation for shallow solitons [18], and is also in agreement with the recent prediction based on the semi-classical Landau dynamics of the dark soliton [17]. On the other hand, to first-order approximation, the radiation (sound waves) emitted by the soliton due to the inhomogeneous background is taken into account. It is shown that radiation plays an important role in the soliton motion, as it is responsible to an anti-damping effect, resulting in the increase of the amplitude of oscillations and decrease of the soliton amplitude. Energy loss of the soliton due to the emission of radiation is approximately found to follow an acceleration-square law, in agreement with previous numerical observations [19]. We have also compared the results of the presented multi-scale expansion technique with the formal perturbation theory for dark solitons. We have found that a formal application of the perturbation theory fails to incorporate the correct dependence of the frequency of the dark soliton oscillation on the soliton amplitude (velocity). Numerical results have been found to be in good agreement to the analytical predictions, within the applicability intervals of the analytical assumptions. Finally, it should be noticed that the presented technique can also be used for the study of dark soliton dynamics in other relevant (inhomogeneous) systems, such as optical lattices and superlattices.

Acknowledgements This work was partially supported by NSF-DMS-0204585, NSF-CAREER, and the Eppley Foundation for Research (PGK) and by NSERC grant (DEP).

-
- [1] Yu.S. Kivshar and B. Luther-Davies, *Phys. Rep.* **298**, 81 (1998).
 - [2] N.P. Proukakis, N.G. Parker, D.J. Frantzeskakis, and C.S. Adams, *J. Opt. B: Quantum Semiclass. Opt.* **6**, S380 (2004).
 - [3] S. Burger, K. Bongs, S. Dettmer, W. Ertmer, K. Sengstock, A. Sanpera, G.V. Shlyapnikov, and M. Lewenstein, *Phys. Rev. Lett.* **83**, 5198 (1999).
 - [4] Z. Dutton, M. Budde, C. Slowe, and L.V. Hau, *Science* **293**, 663 (2001).
 - [5] B.P. Anderson, P.C. Haljan, C.A. Regal, D.L. Feder, L.A. Collins, C.W. Clark, and E.A. Cornell, *Phys. Rev. Lett.* **86**, 2926 (1999).
 - [6] W.P. Reinhardt and C.W. Clark, *J. Phys. B: At. Mol. Opt. Phys.* **30**, L785 (1997).
 - [7] S.A. Morgan, R.J. Ballagh, and K. Burnett, *Phys. Rev. A* **55**, 4338 (1997).
 - [8] Th. Busch and J.R. Anglin, *Phys. Rev. Lett.* **84**, 2298 (2000).
 - [9] D.J. Frantzeskakis, G. Theocharis, F.K. Diakonov, P. Schmelcher, and Yu.S. Kivshar, *Phys. Rev. A* **66**, 053608 (2002).
 - [10] V.A. Brazhnyi and V.V. Konotop, *Phys. Rev. A* **68**, 043613 (2003).
 - [11] V.V. Konotop and V.E. Vekslerchik, *Phys. Rev. E* **49**, 2397 (1994).
 - [12] Yu.S. Kivshar and X. Yang, *Phys. Rev. E* **49**, 1657 (1994).
 - [13] D.E. Pelinovsky, Yu.S. Kivshar, and V.V. Afanasjev, *Phys. Rev. E* **54**, 2015 (1996).
 - [14] X.J. Chen, Z.D. Chen, and N.N. Huang, *J. Phys. A: Math. Gen.* **31**, 6929 (1998).
 - [15] N.N. Huang, S. Chi, and X.J. Chen, *J. Phys. A: Math. Gen.* **32**, 3939 (1999).

- [16] V.M. Lashkin, Phys. Rev. E **70**, 066620 (2004).
- [17] V.V. Konotop and L. Pitaevskii, Phys. Rev. Lett. **93**, 240403 (2004).
- [18] G. Huang, J. Szeftel, and S. Zhu, Phys. Rev. A **65**, 053605 (2002).
- [19] N.G. Parker, N.P. Proukakis, M. Leadbeater, and C.S. Adams, Phys. Rev. Lett. **90**, 220401 (2003).
- [20] N.G. Parker, N.P. Proukakis, M. Leadbeater, and C.S. Adams, J. Phys. B: At. Mol. Opt. Phys. **36**, 2891 (2003).
- [21] N.G. Parker, N.P. Proukakis, C.F. Barengi, and C.S. Adams, J. Phys. B: At. Mol. Opt. Phys. **37**, S175 (2004).
- [22] G. Theocharis, D.J. Frantzeskakis, P.G. Kevrekidis, B.A. Malomed, and Yu.S. Kivshar, Phys. Rev. Lett. **90**, 120403 (2003).
- [23] D.J. Frantzeskakis, N.P. Proukakis, and P.G. Kevrekidis, Phys. Rev. A **70**, 015601 (2004).
- [24] N.P. Proukakis, N.G. Parker, C.F. Barengi, and C.S. Adams, Phys. Rev. Lett. **93**, 130408 (2004).
- [25] N. Bilas and N. Pavloff, preprint cond-mat/0501053.
- [26] V.M. Pérez-García, H. Michinel, and H. Herrero, Phys. Rev. A **57**, 3837 (1998).
- [27] F. Dalfovo, S. Giorgini, L.P. Pitaevskii and S. Stringari, Rev. Mod. Phys. **71**, 463 (1999).
- [28] M. Kurth, SIAM J. Math. Anal. **36**, 967 (2004).
- [29] J.A. Murdock, *Perturbations: Theory and Methods* (SIAM, 1999).
- [30] J. Ockendon, S. Jowison, A. Lacey, and A. Movchan, *Applied Partial Differential Equations* (Cambridge University Press, 1999)